

GRB and Environment Interaction

P. Mészáros¹

¹*Pennsylvania State University, 525 Davey, University Park, PA 16802*

Abstract.

We discuss three aspects of the interaction between GRB and their surroundings. The illumination of the progenitor remnant and/or the surroundings by the X-ray afterglow continuum can produce substantial Fe K-alpha line and edge emission, with implications for the progenitor model. The presence of large dust column densities, capable of obscuring the GRB optical afterglow, will lead to characteristic delayed X-ray and far-IR light curve signatures. Pair production induced by the initial gamma-rays in the nearby environment will modify the initial spectrum and the afterglow light curve, and the magnitude of these changes provides a diagnostic for the external density.

I FE X-RAY LINES FROM GRB PROGENITORS

Important clues for identifying the nature of the progenitors of the long ($t \gtrsim 2$ s) GRBs may be available from the recent report at a 4.7σ level of X-ray Fe line features in the afterglow after 1.5 days of the gamma-ray burst GRB 991216 [10], as well as similar detections at the 3σ level in 5 other bursts with Beppo-SAX and ASCA. X-ray atomic edges and resonance absorption lines are theoretically expected to be detectable from the gas in the immediate environment of the GRB, and in particular from the remnants of a massive progenitor stellar system [15,14,16].

A straightforward interpretation [10] of the GRB 991216 observation would imply a mass $\gtrsim 0.1 - 1M_{\odot}$ of Fe at a distance of about 1-2 light-days, possibly due to a remnant of an explosive event or supernova which occurred days or weeks prior to the gamma-ray burst itself (a 'supranova', [10,12]). The long time delay is necessary both to get the relatively massive, slow moving ejecta out to few light-day distances (to explain the line appearance at a few days with light travel arguments), and in order to get the initial Ni and Co to decay to Fe (~ 55 days). This requires a two-step process, in which an initial supernova leads to a temporarily stabilized neutron star remnant, which after weeks collapses to a black hole leading to a canonical burst ([11,12]). It is unclear whether fall-back from the supernova leading to the second collapse to a BH could occur with such a (\sim weeks) long delay (e.g. [18]). Another possibility is that a massive progenitor has previously emitted a copious wind ($\dot{M} \gtrsim 10^{-4} M_{\odot}/\text{yr}$), which would need to be unusually Fe-rich and highly inhomogeneous ([14]; c.f. [10]).

An alternative, and perhaps less restrictive scenario for such Fe lines [17] involves an extended, possibly magnetically dominated wind from a GRB impacting the expanding envelope of a massive progenitor star. This could be due either to a spinning-down millisecond super-pulsar or to a

highly-magnetised torus around a black hole (e.g. [13]), which could produce a luminosity that was still, one day after the original explosion, as high as $L_m \sim 10^{47} t_{day}^{-1.3}$ ergs. An outflow with such a dependence can also be powered by accretion of fall-back material onto a central black hole [18]. This jet luminosity may not dominate the continuum afterglow; but its impact on the outer portions of the expanding stellar envelope at distances $\lesssim 10^{13}$ cm, even with just solar abundances, can be efficiently reprocessed into an Fe line luminosity comparable to the observed value, together with a contribution to the X-ray continuum. Under this interpretation, the dominant continuum flux in the afterglow, even in the X-ray band, is still attributable to a standard decelerating blast wave.

The relativistic magnetised wind from the compact remnant would develop a stand-off shock before encountering the envelope material, and shocked relativistic plasma would be deflected along the funnel walls. Non-thermal electrons will be accelerated behind the standoff shock in the jet material; the transverse magnetic field strength (which decreases as $1/r$ in an outflowing wind) would be of order 10^4 G at 10^{13} cm – strong enough to ensure that the shock-accelerated electrons cool promptly, yielding a power-law continuum extending into the X-ray band. Some of these X-rays would escape along the funnel, but at least half (the exact proportion depending on the geometry and flow pattern) would irradiate the material in the stellar envelope. Pressure balance in the shocked envelope wall implies densities of $n_e = \alpha L_m / 6\pi r^2 ckT \sim 10^{17} \alpha L_{47} r_{13}^{-2} T_8^{-1} \text{ cm}^{-3}$, where $\alpha \sim 1$ is a geometric factor, and the recombination time for hydrogenic Fe in the funnel walls photoionized by the non-thermal continuum is $t_{rec} = 6 \times 10^{-6} T_8^{1/2} n_{17}^{-1} \sim 6 \times 10^{-6} \alpha L_{m47}^{-1} r_{13}^2 T_8^{3/2} \text{ s}$. Standard calculations of photoionization of optically-thin slabs (e.g. [7]) show that the equivalent width of the Fe K-alpha line, for solar abundances, is about 0.5 keV, or twice as strong if the Fe has ten times solar abundances. These results are applicable provided that the ionizing photons encounter a Fe ion before being scattered by free electrons i.e. provided that $\tau_T = \sigma_T d_i n_e \lesssim 1$. Under these conditions the Fe K- α photon flux is about 0.1 of the X-ray continuum [17], $\dot{N}_{LFe} \sim 10^{54} L_{47} \beta \text{ ph/s}$, where $\beta < 1$ is the ratio of ionizing to MHD luminosity. This line luminosity compares well with Fe line luminosity $6 \times 10^{52} \text{ ph/s}$ observed $t \sim 1.5$ day after the GRB 991216 burst by [10].

The total amount of Fe needed to explain the observed K- α line flux, arising in a thin layer of the funnel walls of a collapsar model, amounts to a very modest mass of $M_{Fe} \sim 10^{-8} M_\odot$, which could be Fe synthesized in the core. The Fe-enriched core material can easily reach a distance comparable to $r \sim 10^{13}$ cm in 1 day for an expansion velocity below the limit $v \sim 10^9 \text{ cm s}^{-1}$ inferred by [10] from the line widths. Even without this, a solar abundance ($10^{-5} M_\odot$ of Fe) in the envelope is sufficient to explain the observations. The initial, energetic portion of the relativistic jet, with a typical burst duration of 1 – 10 s, will rapidly expand beyond the stellar envelope, leading in the usual way to shocks and a decelerating blast wave. A continually decreasing fraction of energy, such as put out by a decaying magnetar, may continue being emitted for periods of a day or longer, and its reprocessing by the stellar envelope can be responsible for the observed Fe line emission in GRB 991216. Since the energy in this tail can decay faster than t^{-1} , the usual standard shock gamma-ray and afterglow scenario need not be affected, being determined by the first 1-10 s worth of the energy input.

II DUSTY GRB DELAYED XR/IR AFTERGLOWS

For GRB in large star forming regions, a significant fraction of the prompt X-ray emission will be scattered by dust grains. Since dust grains scatter X-rays by a small angle, time delays of the scattered x-rays will be small (minutes to days, depending on the X-ray energy and the grain size). If the dust column density is substantial, the softer part of the X-ray afterglow on the above timescales will be dominated by the dust scattering, the direct X-ray emission from the

blast wave being weaker. This intermediate time, soft(er) X-ray light curve will be steeper than the unscattered X-ray afterglow.

As a specific example [6], consider a typical GRB whose unscattered X-ray light curve is parametrized as $F_0(t) = [1 + (t/100\text{s})]/[1 + (t/100\text{s})^{2.3}]$, with an arbitrary normalization depending on the X-ray energy band. This is represented by the thin line in Fig.1. We assume that the GRB occurs in a large star forming region, of typical radius R about 100pc, where the dust grain populations and optical depths are close to what is observed in our Galactic center region. Thus for numerical estimates we assume that (1) visual extinction is ~ 10 , (2) X-rays are scattered preferentially by those dust grains whose size is in the range $a \sim 0.06\mu\text{m}$, (3) the optical depth to dust scattering at the X-ray energy ϵ is $\tau(\epsilon) = 3 \left(\frac{\epsilon}{1\text{keV}}\right)^{-2}$. At X-ray optical depths less than few, dust grains of size a will scatter X-rays of energy ϵ by an angle $\theta \sim 0.2\lambda/a$, where λ is the X-ray wavelength, $\theta(\epsilon) \simeq 4 \times 10^{-3} \left(\frac{a}{0.06\mu\text{m}}\right)^{-1} \left(\frac{\epsilon}{1\text{keV}}\right)^{-1}$. The time lag is $t \sim R\theta^2/2c$, or $t(\epsilon) \sim 9 \times 10^4\text{s} \left(\frac{a}{0.06\mu\text{m}}\right)^{-2} \left(\frac{\epsilon}{1\text{keV}}\right)^{-2} \left(\frac{R}{100\text{pc}}\right)$.

At 2 keV, the optical depth is $\tau \sim 1$. The time lag is $t \sim 2 \times 10^4\text{s}$. The scattered flux is $F_s \sim \tau f/t \sim 0.03$. The unscattered flux at $2 \times 10^4\text{s}$ is $F_0 \sim 10^{-3}$. In the time interval from hours to weeks, the dust scattering dominates the afterglow, and, as shown in Fig.1, the afterglow is approximately a power law $F \propto t^{-1.75}$ [6]. This is because dust grains of radius $a < 0.06\mu\text{m}$ will scatter the prompt emission with longer time lags, $t \propto a^{-2}$, and with smaller optical depths τ . To calculate τ , we take a standard dust grain size distribution where the number of grains of size of order a is $\propto a^{-2.5}$. For a scattering cross section $\propto a^4$ the optical depth is $\tau \propto a^{1.5} \propto t^{-0.75}$, so the flux $F \propto t^{-1.75}$.

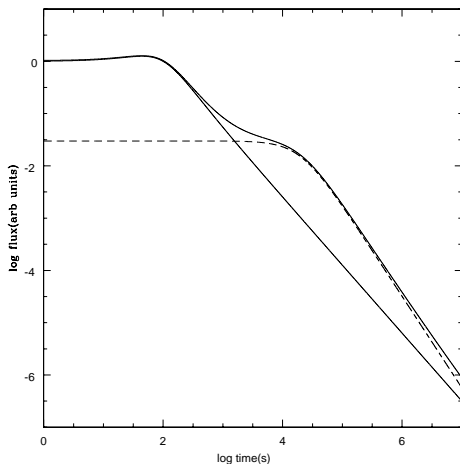


FIGURE 1. Dust-scattered X-ray afterglow. Thin line: unscattered X-ray flux. Thin dashed line: scattered X-ray flux. Thick line: total flux. The flux normalization is arbitrary, the relative fluxes correspond to the example discussed in the text for an energy of 2 keV [6].

A GRB in such a highly obscured star-forming region should lead to specific signatures in the X-ray afterglow, i.e. a bump in the X-ray light curve at energies $\epsilon \sim 2 - 3$ keV, hours to days after the burst [6]. This X-ray signature is expected for bursts which do not produce a detectable optical transient (OT). Such OT-less, X-ray peculiar GRBs will also lead to thermal reemission and scattering of the O/UV flux causing a delayed IR emission, as is the case also for partially absorbed bursts [8,9]. For an isotropic total burst energy $E \sim 10^{53}$ erg at a redshift $z \sim 1$ the normalization of the X-ray flux for the burst of Figure 1 would be $F_x \sim 10^{-9}$ erg cm^{-2} s^{-1} keV^{-1} for $t \lesssim 100$ s, in the usual range of X-ray afterglow fluxes detected by Beppo-SAX. The dust reradiation occurs beyond the sublimation radius $R_s \sim 10 L_{49}^{1/2}$ pc at wavelengths $\lambda \gtrsim 2(1+z)\mu\text{m}$, where $10^{49} L_{49}$ erg/s is the early UV component of burst afterglow [8]. The time delay associated

with the reradiated flux is $t_{IR} \sim (R_s/2c)\theta_j^2$ where $\theta_j = 10^{-1}\theta_{-1}$. At $z \sim 1$ the corresponding infrared flux at $2.2 \mu\text{m}$ would be $F_{2.2\mu\text{m}} \sim L_{49}\theta_j^2/[4\pi D_L^2(R_s/2c)\theta_j^2\nu] \sim 0.3L_{49}^{1/2} \mu\text{Jy}$, independent of θ_j , or $m_K \sim 23.3$ compared to Vega [6], approximately constant for a time $t_{IR} \sim 5 \times 10^6 \theta_{-1}^2 L_{49}^{1/2}$ s. Such γ -ray detected GRBs with anomalous X-ray afterglow behavior and no OT may be used as tracers of massive stellar collapses. It may thus be possible to detect star-forming regions out to redshifts larger than achievable with O/IR techniques, since typical GRB γ -ray, X-ray and IR fluxes can in principle be measured out to $z \sim 10 - 15$.

III PAIR PRODUCTION IN GRB ENVIRONMENTS

Gamma-ray burst sources with a high luminosity can produce e^\pm pair cascades in their environment as a result of back-scattering of a seed fraction of their original hard spectrum. New pairs can be made as some of the initial energetic photons are backscattered and interact with other incoming photons. Previous work on this investigated the acceleration of new pairs for a particular fireball model [1,4], the effect of pair formation for a low compactness parameter external shock model of GRB [3], and Compton echos produced by pairs [2]. Here we discuss a simplified analytical treatment [5] of pair effects from γ -rays arising in internal shocks in a wind; the remaining wind energy drives a blast wave which decelerates as it sweeps up the external medium, and gives rise to the afterglow emission. The γ -rays would propagate ahead of the blast wave, leading to pair production (and an associated deposition of momentum) into the external medium. The pair cascades saturate after the external (pair-enriched) medium reaches a critical bulk Lorentz factor, which is generally below that of the original relativistic wind. For external baryonic densities similar to those in molecular clouds the pairs can achieve scattering optical depths $\tau_\pm \lesssim 1$. Even for less extreme external densities the effect of the additional pairs can be substantial, increasing the radiative efficiency of the blast wave and leading to distortions of the original spectrum. This provides a potential tool for diagnosing the compactness parameter of the bursts and thus the radial distance at which shocks can occur. It also provides a tool for diagnosing the baryonic density of the external environment, and testing the association with star-forming regions.

For the maximum Lorentz factor to which an e^\pm can be accelerated by scattering, and the maximum Lorentz factor at which back-scattered photons can still make new pairs, one finds two regimes defined by the effective duration of the light pulse seen by the screen of accelerated pairs. At low radii (wind regime) the effective duration is the burst duration t_w ; for large radii (impulsive regime), the effective duration is $\Delta t \sim r/c\Gamma_\pm^2$. For an incident photon number index $\beta = 2$, in the former $\Gamma_\pm \propto r^{-1/3}$ and in the latter $\Gamma_\pm \propto r^{-2}$. The critical radius and Lorentz factor for the transition between the wind and the impulsive regimes are [5] $r_c = 5 \times 10^{14} L_{w50}^{2/5} t_{w1}^{3/5}$, $\Gamma_c = 3 \times 10^1 L_{w50}^{1/5} t_{w1}^{-1/5}$. The maximum radius at which pair cascades cut off is $r_\ell \sim (4r_* ct_w/3)^{1/2} \sim 4 \times 10^{15} L_{w50}^{1/2} t_{w1}^{1/2}$ cm. Before the pairs start accelerating, assuming they are held back by the environmental protons through magnetic fields, an initial cascade amplification factor $k_p \sim (m_p/m_e)$ is achieved. After the mean mass per scatterer drops to a value comparable to the electron mass, before reaching r_ℓ a further amplification $k_a \sim 2^s \sim 50$ (where $s \sim \log \Gamma_c / \log 2$) is possible, so the total pair amplification factor is [5] $k_c = k_p k_a(r_c) \sim (m_p/m_e)\Gamma_c \sim 5 \times 10^4 L_{w50}^{1/5} t_{w1}^{-1/5}$. The maximum pair optical depth at r_c , which is prevented from exceeding $\tau_\pm \sim 1$ by self-shielding, is achieved for external densities $n_p \gtrsim n_{p,c}$, where $n_{p,c} \simeq 10^5 L_{w50}^{-3/5} t_{w1}^{-2/5} \text{ cm}^{-3}$.

The external density and the initial Lorentz factor η determine when the outer shock and the reverse shock become important and whether this happens within the radius already polluted with pairs. If $\eta \lesssim r_l/ct_w$ the external shock responsible for the afterglow occurs beyond the region

“polluted” by new pairs, and otherwise the afterglow shock may experience, after starting out in the canonical manner, a “resurgence” or second kick as its radiative efficiency is boosted by running into an e^\pm -enriched gas [5].

Additional effects are expected when $\tau_\pm \rightarrow 1$, for external baryon density $n_p \gtrsim n_{c,p} \sim 10^5 L_{w50}^{-2/5} t_{w1}^{-3/5} \text{cm}^{-3}$ at radii $r < r_\ell$. Such high densities could be expected if the burst is associated with a massive star in which prior mass loss led to a dense circumstellar envelope. The pair optical depth saturates to $\tau_\pm \sim 1$ and in addition to an increased efficiency and softer spectrum of the afterglow reverse shock, the original gamma-ray spectrum of the GRB will be modified as well. One of the consequences of such a critical external density leading to $\tau_\pm \sim 1$ would be the presence of an X-ray quasi-thermal pulse, whose total energy may be a few percent of the total burst energy [5].

This research was supported by NASA NAG5-9192, the Guggenheim Foundation and the Sackler Foundation. I am grateful to M.J. Rees, A. Gruzinov and E. Ramirez-Ruiz for valuable discussions on these topics.

REFERENCES

1. Madau, P & Thompson, C, 2000 ApJ, 534, 239
2. Madau, P, Blandford, R & Rees, M.J., 2000, ApJ, 541, 712.
3. Dermer, C & Böttcher, M., 2000 ApJ 534, L155
4. Thompson, C & Madau, P, 2000 ApJ, 538, 105
5. Mészáros, P, Ramirez-Ruiz, E & Rees, M, 2001, ApJ subm(astro-ph/0011284)
6. Mészáros, P & Gruzinov, A, 2000, ApJL, 543, L35 (astro-ph/0007255)
7. Young, A.J., 1999, Ph.D. thesis, Cambridge University
8. Waxman, E & Draine, B., 2000, ApJ, in press (astro-ph/9909020)
9. Esin, A & Blandford, R.D., 2000, ApJL in press (astro-ph/0003415)
10. Piro, L, et al., 2000, Science, 290, 955)
11. Vietri, M & Stella, L.A., 1998, ApJ 507, L45
12. Vietri, M, Perola, G, Piro, L & Stella, L, 2000, MNRAS 308, L29.
13. Wheeler, J.C, et al., 2000, ApJ in press (astro-ph/9909293)
14. Weth, C, Mészáros, P, Kallman, T & Rees, M.J, 2000, ApJ 534, 581
15. Mészáros, P & Rees, M.J. 1998, MNRAS, 299, L10
16. Böttcher, M & Fryer, C.L, 2000, ApJ, subm. (astro-ph/0006076)
17. Rees, M.J. & Mészáros, P, 2000, ApJ, 545, L73
18. MacFadyen, A, Woosley, S & Heger, A, 2000, ApJ(astro-ph/9910034)